Title
Evaluation of Doxorubicin-Loaded 3-Helix Micelles as Nanocarriers

Journal
Biomacromolecules, 14(10)

ISSN
1525-7797

Authors
Dube, Nikhil
Shu, Jessica Y
Dong, He
et al.

Publication Date
2013-10-14

DOI
10.1021/bm4010518

Peer reviewed

Published in final edited form as:
Biomacromolecules. 2013 October 14; 14(10): 3697–3705. doi:10.1021/bm4010518.

Evaluation of Doxorubicin-loaded 3-Helix Micelles as Nanocarriers

Nikhil Dube[a], **Jessica Y. Shu**[a], **He Dong**[a], **Jai W. Seo**[b], **Elizabeth Ingham**[b], **Azadeh Kheirolomoom**[b], **Pin-Yuan Chen**[c], **John Forsayeth**[c], **Krystof Bankiewicz**[c], **Katherine W. Ferrara**[b], and **Ting Xu**[a,d,e,*]

[a]Department of Materials Science & Engineering, University of California, Berkeley, California 94720, United States

[b]Department of Biomedical Engineering, University of California, Davis, California 95616, United States

[c]Department of Neurosurgery, University of California San Francisco, San Francisco, California 94103, United States

[d]Department of Chemistry, University of California, Berkeley, California 94720, United States

[e]Materials Science Division, Lawrence Berkeley National Laboratory, Berkeley, California 94720, United States

Abstract

Designing stable drug nanocarriers, 10-30 nm in size, would have significant impact on their transport in circulation, tumor penetration and therapeutic efficacy. In the present study, biological properties of 3-helix micelles loaded with 8 wt% doxorubicin (DOX), ~15 nm in size, were characterized to validate their potential as a nanocarrier platform. DOX-loaded micelles exhibited high stability in terms of size and drug retention in concentrated protein environments similar to conditions after intravenous injections. DOX-loaded micelles were cytotoxic to PPC-1 and 4T1 cancer cells at levels comparable to free DOX. 3-helix micelles can be disassembled by proteolytic degradation of peptide shell to enable drug release and clearance to minimize long-term accumulation. Local administration to normal rat striatum by convection enhanced delivery (CED) showed greater extent of drug distribution and reduced toxicity relative to free drug. Intravenous administration of DOX-loaded 3-helix micelles demonstrated improved tumor half-life and reduced toxicity to healthy tissues in comparison to free DOX. *In vivo* delivery of DOX-loaded 3-helix micelles through two different routes clearly indicates the potential of 3-helix micelles as safe and effective nanocarriers for cancer therapeutics.

Keywords

Dox-loaded 3-helix micelles; Biological Stability; Cytotoxicity; Biodistribution; Off-Target Accumulation

[*]Corresponding Author: tingxu@berkeley.edu, Phone: 510-642-1632, Fax: 510-643-5792.

Supplementary Information **Available:** Structural characterization of 3-helix micelles with different DOX loading content is provided. This information is available free of charge via the Internet at http://pubs.acs.org.

1. Introduction

Improved understanding of the effect of different physicochemical parameters of nanoparticles on their biological performance has facilitated the progress of a number of nanocarrier platforms to advanced stages in clinical development.[1-9] Critical requirements for clinical success of drug nanocarriers intended for intravenous administration are reproducible drug loadings in significant quantity, aqueous solubility of the formulation, stability in blood circulation with high retention of encapsulated agent, accumulation at the disease site, controlled drug release from the carrier and minimal toxicity to healthy tissues. Nanoparticle size has a critical effect on their transport in blood circulation and within tumor.[10-13] Smaller nanoparticles, 10-30 nm in size, have been shown to rapidly diffuse throughout the tumor matrix[10-12] and exhibit greater extent of cellular accumulation and faster internalization in cancer cells.[14-16] Recent studies on small nanocarriers, 10-30 nm in size, based on dendrimers[17] and peptide micelles[18] with chemically conjugated anticancer drugs have shown enhanced therapeutic effect after a single intravenous administration in C-26 colon carcinoma-bearing mice. These findings suggest that drug nanocarriers in the range of 10-30 nm, with high stability, and better tumor accumulation offer the opportunity to achieve optimal therapeutic efficacy.

We recently developed long circulating spherical nanocarriers, called “3-helix micelles”, ~ 15 nm in size, based on amphiphilic peptide-PEG conjugates where the head-group self-associates into a coiled-coil 3-helix bundle.[19, 20] Coiled-coils are one of tertiary structure motifs commonly found in natural proteins.[21, 22] Our micelle design is based on an amphiphilic subunit that consists of a coiled-coil forming peptide with a PEG chain covalently attached to the exterior of the coiled-coil and hydrophobic stearic acid tails attached to the N-terminus (see supporting information for detailed amphiphile structure). The protein tertiary structure allows to position entropic repulsive interactions between PEG chains in the headgroup to stabilize individual micelles.[20] 3-helix micelles, despite of their small size, have demonstrated good *in vivo* stability with reduced accumulation in liver and spleen.[19] In comparison to dendrimer,[5, 23] 3-helix micelles are constructed via self-assembly and can eventually disassociate and degrade into biocompatible subunits to be cleared through kidney to reduce long-term side effect. It is critical that stability is maintained after drug incorporation as premature drug release from the formulation may lead to systemic side effects and reduced drug efficacy. Previous cargo leakage studies of 3-helix micelles are mostly based on dye molecules used for fluorescent labeling of micelles for analytical studies.[19] Maintaining stability of nanocarrier loaded with clinically relevant drugs in protein rich environments encountered in blood circulation after intravenous administration is important.[24-26] Evaluation of the stability of encapsulated drug in plasma relevant conditions is critical for accurate prediction of circulation stability, biodistribution and tissue half-life of drug-loaded carriers. For drug nanocarriers stable in circulation, triggered release of drug at disease site is an equally critical requirement for therapeutic efficacy. Nanocarriers have been designed to release drugs in response to disease specific environmental triggers such as pH[5, 17, 18, 27] and proteases.[28, 29] 3-helix micelles with their peptide based shell provide an attractive platform where drug release could potentially be triggered by proteolytic degradation.

We used doxorubicin (DOX) as the model anticancer drug, to undertake a systematic *in vitro* and *in vivo* validation of 3-helix micelles as a viable drug carrier. Drug loaded micelles could be reproducibly formulated in aqueous buffer with 8 wt% DOX content without any adverse effects on the size and core-shell structure of the micelles. We establish that DOX-loaded 3-helix micelles meet important requirements in terms of drug loading, excellent stability in protein rich biological environments with minimum cargo leakage, high cytotoxicity towards cancer cells, and sensitivity to proteolytic degradation to enable

intracellular drug release and ensure clearance to minimize off-target side effects. Micelles could be disassembled by protease-mediated degradation of peptide based micellar shell, which is critical for drug release and clearance to minimize side effects. DOX-loaded micelles were cytotoxic to a range of cancer cells confirming the release of active drug from micelles. Localized delivery of DOX-loaded micelles to rat brain by convection-enhanced delivery (CED) indicated greater biodistribution and significantly reduced toxicity of drug encapsulated in micelle compared to free drug. Intravenous administration of DOX-loaded micelles indicated selective tumor localization at 72 h after injection, and resulted in reduced toxicity to healthy tissues. These studies established that drug half-life and toxicity of DOX-loaded micelles are favorably altered relative to free drug. The present study clearly indicates the potential of 3-helix micelles as a viable nanocarrier platform that meets many critical requirements for drug formulation.

2. Experimental Section

2.1 Synthesis of Peptide-Polymer Conjugate

The design of amphiphile is based on a 3-helix bundle peptide designed *de novo*, 1coi (EVEALEKKVAALECKVQALEKKVEALEHGW).[30, 31] The peptide was synthesized on a Prelude solid-phase synthesizer (Protein Technologies) using standard 9-fluorenylmethyl carbamate (Fmoc) chemistry. The details about materials and the synthesis of amphiphilic peptide-polymer conjugate have been described previously.[19] The conjugate is referred as dC18-1coi(P2K)-P750. Detailed synthesis and purification can be found in ref. 19 and is provided in the supporting information. The purity of conjugate as determined is ~ 90%.

2.2. Loading of DOX in 3-Helix Micelles

DOX was loaded into micelles by thin film hydration method. 1 mg dC18-1coi(P2K)-P750 and 0.1 mg of DOX were dissolved in 0.5 ml of methanol in a glass vial and the solvent was evaporated in vacuum oven for 3 h. The dried film containing the conjugate and drug was rehydrated with 0.5 ml of 25 mM phosphate buffer, pH 7.4, and the solution was stirred for 16 h to allow assembly into drug loaded 3-helix micelles. Free unencapsulated drug was removed by centrifugation at 14000 RPM for 3 minutes. The supernatant was transferred into centrifugal filters (Amicon, MW cutoff: 3000 Da) for spin ultrafiltration to remove any free dissolved drug. Spin filtration was performed at 7500 RPM for 30 minutes and was done three times. The concentrate was washed with water and lyophilized to obtain DOX-loaded micelles as a dry red powder. DOX-loaded micelles were dissolved in methanol and loading was determined by absorbance of DOX at 480 nm. Absorbance of 0.2 mg/ml of DOX-loaded micelles dissolved in methanol was used to calculate DOX loading. The molar extinction coefficient for DOX obtained by the standard curve for absorbance of DOX dissolved in methanol was calculated to be ~ 11337.8 $M^{-1}cm^{-1}$. The details of the calculations are described in supporting information. Maximum DOX loading obtained was 8 wt%. For all experiments, lyophilized powder of DOX-loaded micelles was dissolved in 25 mM phosphate buffer, pH 7.4.

2.3. Structural Characterization of DOX-loaded 3-Helix Micelles

Size exclusion chromatography (SEC) was carried out on a BioSep-SEC-S 4000 column (Phenomenex). The flow rate was 1 ml/min with 25 mM phosphate buffer, pH 7.4, as the elution solvent. The elution profile was monitored with a UV-Vis detector at wavelengths of 220 nm and 480 nm. Dynamic Light Scattering (DLS) size measurements on drug loaded micelles were made on a Malvern Zetasizer Nano-ZS with a 633 nm laser and a scattering angle of 17°. Refractive index of 1.45 was used for the measurements. FEI Tecnai 12 transmission electron microscope (TEM) at 120 kV was used to study the morphology of DOX-loaded micelles. DOX-loaded micelles solution (5 μl, 0.2 mg/ml) was dropped onto a

discharged holey carbon coated grid (Ted Pella 01824), followed by phosphotungstic acid (5 μl, 2 wt %, pH 3.3) solution. Circular dichroism (CD) measurements were made on a Jasco J810 spectropolarimeter from 260 to 190 nm at 0.2 nm intervals, a rate of a 100 nm/min, a response time of 4 s, and a bandwidth of 1 nm. Differential Scanning Calorimetry (DSC) was performed on a VP-MicroCal (GE). Both blank and DOX-loaded micelles (600 μl, 2 mg/ml) dissolved in phosphate buffer, pH 7.4, were analyzed, as temperature was increased from 5 °C to 60 °C at a rate of 1 °C/min. DSC thermograms were obtained after concentration normalization and baseline correction with Origin software provided by MicroCal. The enthalpy change associated with alkyl chain phase transition was calculated by using area under the curve function in Igor Pro 6.

2.4. Stability and DOX Release in Serum Albumin

DOX-loaded micelles (10 mg/ml) and serum albumin (10 mg/ml) were mixed and incubated at 37 °C for 20 hours and the mixture was analyzed by SEC for any changes in size distribution. The release of DOX from 3-helix micelles was monitored by change in fluorescence of DOX-loaded micelles in presence of serum albumin (50 mg/ml). Fluorescence measurements were performed on LS-55 fluorometer (Perkin Elmer). Micelle solution in quartz cuvettes was excited at 480 nm and the emission spectra were recorded from 510-650 nm for 20 hours.

2.5. Proteolytic Disassembly of 3-Helix Micelles

Fluorescence recovery of fluorescein labeled 3-helix micelles in presence of proteinase K was monitored to study proteolytic disassembly of micelles. 10 μl of concentrated proteinase K (final concentration: 150 μg/ml) was added to fluorescently quenched solution of dye labeled micelles (15 μM peptide, 30 mol% fluorescein, 90 μl). The final molar ratio of proteinase K to peptide in solution was 1:27. The increase in fluorescence after addition of protease was monitored for 3 hours. Fluorescein was excited at 480 nm and emission spectra were recorded from 490-640 nm. The degradation of peptide in the micellar shell was analyzed by mass spectroscopy. 1 μl of sample was mixed with 1 μl of 10 mg/ml α-cyano-4-hydroxycinnamic acid matrix in acetonitrile and spotted on stainless steel MALDI plate. The spot was allowed to dry for 5 minutes and the spectrum were collected on MALDI-TOF spectrometer (Applied BioSystems)

2.6. In Vitro Cytotoxicity

Cytotoxicity of free DOX, blank micelles and DOX-loaded micelles was investigated by MTT assay. Two widely different cell lines were chosen in order to confirm the functionality of DOX-loaded micelles in releasing active doxorubicin once internalized in a range of cancer cell types. PPC-1 is a human line and 4T1 is syngenic mouse line and both of the cells are highly metastatic. Both express markers such as neuropilin-1 but otherwise have differences in species of origin and in organ of origin. PPC-1 and 4T1 cells were cultured in DMEM high glucose medium containing 10% FBS and IMDM medium containing 10% FBS respectively. 1% Penicillin-Streptomycin (10,000 Units/mL and 10,000 ug/mL respectively) was added to all culture media. 24 h before experiments, cells were seeded at 2000 cells/well in 96-well tissue culture plates. Treatments were added in 100 μl medium/well in triplicate: 1) 25% PBS (v/v) in medium, 2) free DOX (1 μg/ml and 5 μg/ml), 3) DOX-loaded micelles (1 μg/ml and 5 μg/ml encapsulated DOX) and 4) blank micelles (concentration matched to the peptide content of the DOX-loaded micelles at DOX concentration of 5 μg/ml). After 36 to 72 h continuous incubation of cells with each treatment at 37°C in 5% CO2, cytotoxicity was quantified via MTT assay. MTT reagent (3-(4,5-dimethylthiazol-2-yl)-2,5-diphenyltetrazolium bromide, 100 μl, 1.2 mM) was added to each well, and cells were incubated for 2 h at 37°C in 5% CO_2. After removal of medium, formazan crystals were dissolved in DMSO (100 μl/well) and absorbance was measured at

wavelength 570 nm using a Tecan (San Jose, CA) Infinite® M1000 microplate reader. Treatments were tested in triplicate and two independent replicates of each MTT assay were performed. Statistical comparisons were performed by ANOVA followed by Tukey's multiple comparisons test. p-values of less than 0.05 were considered significant (* $p < 0.05$, ** $p < 0.0001$).

2.7. Convection-Enhanced Delivery (CED) of Micelles

3-helix micelles were administered to rat brain by CED to examine their distribution within the brain tissue. All procedures were in accordance with the regulations of the Institutional Animal Care and Use Committee of the University of California at San Francisco. 20 μl of free DOX and DOX-loaded micelles (DOX concentration: 0.2 mg/ml) were infused by CED at a rate of 0.5 μl/min in the striatum of normal Sprague Dawley rats as previously described[32]. Briefly, after rats were anesthetized, a sagittal incision was made in the skin, and burr-holes were made in the skull by a drill. To minimize trauma and reflux, silica cannulae (O.D. 235 μm; ID. 100 μm) were used for all infusions (Polymicro Technologies, Phoenix, AZ). The cannulae were attached directly to Nanofill-100 syringes placed in the pumps controlled by a Micro4™ MicroSyringe Pump Controller (World Precision Instrument). The coordinates for the injection were taken from the rat brain atlas [33]. A week after infusion, the rats were euthanized and brain tissue was sectioned and distribution of micelles was examined with optical microscope. The tissue sections were stained with hematoxylin and eosin (H&E) to look for pathology.

2.8. Intravenous Administration of DOX-loaded Micelles

All animal experiments for intravenous administration were conducted under a protocol approved by the University of California, Davis, Institutional Animal Care and Use Committee (Davis, CA). NDL tumors were transplanted into the inguinal mammary fat fads of five to six week old FVB mice.[34] Approximately after 3 weeks, when the size range of the NDL tumors was 5-10 mm, animals were anesthetized with isoflurane and received an intravenous (IV) injection of DOX-loaded micelles. 150 μl of DOX-loaded micelles at a concentration of 12 mg/ml was injected. Mice were euthanized with an IV injection of Euthasol (Western Medical Supply, CA) at 24 h and 72 h after administration. Blood was drawn and 50 ml of saline was perfused into the left ventricle. Organs of interest, such as heart, liver, spleen, kidneys, skin, and tumors, were harvested and scanned on a Maestro 2 imaging system (PerkinElmer, Massachusetts). Images were acquired at emission wavelength of 550 nm. For skin toxicity assay, DOX-loaded micelles (6mg DOX/kg) were administered to mice intravenously two times per week. Images were taken at three weeks after treatment started. Skin toxicity from DOX-loaded micelles was compared with the treatment from Doxil as previously reported.[35]

3. Results and Discussion

3.1. DOX loading in 3-helix micelles

DOX is a highly potent anticancer drug and its efficacy in a variety of *in vivo* tumor models as well as in humans is well documented.[36] However, the use of DOX is severely limited by its poor aqueous solubility, stability and high cardiotoxicity.[37, 38] There have been a number of studies focused on the design of nanocarrier based DOX formulations to evaluate their potential as safe and effective anticancer therapeutics.[17, 39-46] Hence, DOX is a good model drug to explore the potential of 3-helix micelles as a nanocarrier platform.

The highest DOX loading that could be obtained in 3-helix micelles is ~ 8 wt%. Micelles with different DOX loadings were prepared to investigate the effect of drug content on micelle structure. Fluorescence of DOX in micelles is significantly reduced compared to

fluorescence of free drug at the same concentration due to self-quenching of drug molecules in close proximity with each other, which indicates encapsulation of drug in micelles (Fig. SI1). DLS and SEC (Figs. SI2 and SI3) show that the size of DOX-loaded micelles is ~ 15 nm with uniform size distribution, similar to empty micelles without DOX. The distribution of size by number, volume and intensity measured by DLS confirm that micelles with different DOX loading content are similar in terms of size and uniformity of distribution (Figs. SI4A, SI4B and SI4C). Negatively stained TEM (Fig. 1A), provided further evidence that assembly of 3-helix micelles is maintained in presence of DOX. CD (Fig. SI5) indicates α-helical conformation of peptide, and the ellipticity ratio of 1.04 suggests that the coiled-coil tertiary structure of the peptide is maintained after incorporation of DOX. Fig. 1B shows DSC thermograms for DOX-loaded micelles and unloaded micelles. For unloaded micelles, the endothermic peak with a transition temperature ~24 °C, corresponds to the melting of alkyl chain packing in the micelle core. The transition temperature for the DOX-loaded micelles is increased to ~ 33 °C, which indicates interaction of DOX with stearic acid in the micelle core. The enthalpy change associated with transition in unloaded micelles is 0.674 Cal/g, and that for DOX-loaded micelles is 0.474 Cal/g. These results indicate the formation of a distinct thermodynamic phase in the core of DOX-loaded micelles, different from the core of empty micelles, possibly formed by the co-assembly of drug with alkyl chains. Based on these studies, it is evident that aqueous solubility, size and uniformity of size distribution and core-shell structure of 3-helix micelles are maintained after incorporation of DOX at significant loading content.

The drug loading capacity of micelles is primarily determined by the chemical compatibility of the drug with micellar core.[47-49] However, geometrical factors especially, micellar core size and molecular volume of drug, are critical in determining the drug capacity of micelles. DOX loadings in the range of 12-15 wt% have been reported for block copolymer micelles, 30-40 nm in size.[40, 41, 43, 50] The core volume of these micelles is larger compared to the alkyl chain based core of 3-helix micelles. The maximum DOX loading that could be achieved in 3-helix micelles was ~ 8 wt%, which is comparable to nanocarriers that have demonstrated high *in vivo* efficacy.[17, 18]

3.2. Stability and drug retention of DOX-loaded micelles under physiological conditions

Resistance to nonspecific protein adsorption and retention of therapeutic agent are critical requirements for stable nanocarriers to achieve extended blood circulation after intravenous administration with minimum cargo leakage. The stability of DOX-loaded 3-helix micelles was investigated in presence of serum albumin under physiological conditions. Fig. 2A shows the SEC chromatogram of DOX-loaded micelles incubated in serum albumin for 20 h at 37°C. The chromatograms of serum albumin and fresh DOX-loaded micelles indicate distinct elution profiles for the two components. The overlapping signals monitored at 220 nm and 480 nm for DOX-loaded micelles confirm the encapsulation of DOX in 3-helix micelles. After incubation of DOX-loaded micelles with serum albumin for 20 h, the chromatogram shows minimal differences from the chromatograms of the individual components. This confirms that the size and the uniformity of size distribution of DOX-loaded micelles are not significantly altered in protein rich biological environment. The encapsulation stability of drug within the micelle was investigated in presence of albumin, by monitoring fluorescence of DOX-loaded micelles over time. Fig. 2B shows a very gradual change in the fluorescence of DOX-loaded micelles in presence of serum albumin for 20 h. The emission spectrum of an equivalent amount of DOX-loaded micelles dissolved in methanol is shown as a reference for fluorescence intensity from the free drug as methanol disrupts the structure of micelles. The inset in Fig. 2B reveals a slow rate of recovery for DOX fluorescence, only 12% after 20 hours, which suggests stable encapsulation of DOX in micelles with slow release in presence of serum albumin.

Quantification by dialysis bag release confirmed slow and extended release, with ~ 11% DOX released from 3-helix micelles after 20 hours. DOX-loaded block copolymer micelles, 30-50 nm in size, have shown high encapsulation stability with ~ 20% drug release in 24 hours.[40, 42, 51] Shell-crosslinked micelles, where the polymeric shell is covalently crosslinked to stabilize the micelles have been reported as nanocarriers for DOX formulation. These micelles, 17-50 nm in size, exhibit slow drug release, ~ 40% in 24 hours, and the burst release due to loosely associated drug close to micelle surface is small.[44, 50] The slow *in vitro* DOX release from 3-helix micelles in concentrated serum albumin is comparable to reported studies, but the features like smaller size and clearance of 3-helix micelles may offer more advantages as nanocarrier. These results indicate stable drug encapsulation in 3-helix micelles and are promising for their application in drug formulation. The results from these studies indicate high resistance of DOX-loaded 3-helix micelles towards nonspecific protein adsorption and extended drug retention in highly concentrated protein environments mimicking conditions after intravenous administration.

3.3. Cytotoxicity of DOX-loaded 3-helix micelles

In addition to cargo stability during transport, an equally important requirement for effective anticancer nanocarriers is to control drug release at the disease site after tumor localization and/or cellular internalization. For stable nanocarriers, the modulated cargo release is critical to ensure antitumor effect. MTT assay showed that DOX-loaded micelles exhibited concentration and time dependent *in vitro* cytotoxicity towards PPC-1 and 4T1 cancer cells (Fig. 3). DOX-loaded micelles effectively suppressed the growth of these cancer cells by 36 h and the rate and extent of cytotoxicity was comparable to that of free DOX. These results confirm DOX release from 3-helix micelles in active form. Lower toxicity from DOX loaded nanocarriers, relative to free DOX has been observed for particles larger than 25 nm, after similar incubation times of 72 hours.[18, 42, 43, 45, 46] The slower intracellular drug release and the resulting lower toxicity from nanocarriers is attributed to the size dependent mechanisms of cellular uptake, drug release and subsequent localization of DOX in target cell nucleus. In contrast, free DOX can diffuse rapidly through the lipid bilayer into the cell and nucleus. The toxicity of DOX-loaded 3-helix micelles to cancer cells is comparable to free DOX after 72 hours, which is encouraging for therapeutic potential of this system.

3.4 Proteolytic degradation of 3-helix micelles

On the basis of stability studies, there is negligible drug release from micelles in cell culture medium and thus, the high toxicity of DOX-loaded micelles is due to release of DOX after cellular internalization. We hypothesize that the 3-helix peptide should be cleavable by proteolytic degradation. 3-helix micelles were incubated with proteinase K, a broad spectrum protease that cleaves peptide bonds adjacent to carboxyl group of aliphatic and aromatic amino acids. The sequence of 1coi peptide shows multiple sites of proteolytic cleavage by proteinase K. MALDI spectrum of a micelle solution shows a peak at ~ 7200 Da, the mass of the amphiphilic building block, dC18-1coi(P2K)-P750 (Fig. 4A). MALDI spectrum of micelles incubated with proteinase K indicates the disappearance of amphiphile peak and the appearance of peaks associated with PEG chains attached to small peptide fragments, which suggests degradation of peptide. Based on the potential cleavage sites of proteinase K, we speculate the peptide fragments connected to polymer chains as GGGK-P750 and ECKV-PEG2K, after proteolytic degradation of 3-helix micelles. In order to confirm micelle disassembly under proteolytic conditions, fluorescence of dye labeled micelles was monitored in presence of proteinase K. For this study, 3-helix micelles were labeled with fluorescein that self quenches when placed closed to other fluorescein molecules. Fig. 4B shows that the emission intensity of fluorescein labeled micelles is significantly lower compared to free fluorescein in solution at the same concentration due to self-quenching of dye fluorescence on the micelle surface. After addition of proteinase K,

fluorescence intensity starts to increase potentially due to degradation of peptide in the micellar shell, which leads to fluorescence recovery of the quenched dye. These results confirm the proteolytic degradation of peptide in micellar shell and subsequent disassembly of 3-helix micelles. 3-helix micelles undergo proteolytic disassembly after cellular internalization, resulting in DOX release that leads to cytotoxicity as demonstrated by MTT assay. The disassembly of 3- helix micelles can be triggered by proteases for drug release and clearance to minimize side effects. This unique feature opens new opportunities to design micelles where drug release can be triggered in response to tumor-specific proteases.

3.5. Convection-enhanced delivery (CED) of DOX-loaded micelles

CED is a pressurized infusion technique that allows even distribution of therapeutic agents at high concentrations over a larger area in brain tissue, than in the absence of CED, i.e. by diffusion alone. Anatomical targeting by direct infusion via CED obviates the need for active targeting since restriction of infusate within the tumor margins provides most of the specificity needed and eliminates systemic toxicity. However, the frequency with which CED infusions can be performed into brain tumors is necessarily limited. There is a critical need to develop drug nanocarriers with long tissue-half lives and extended drug release that can be delivered by CED to brain tumors. We have previously used this procedure to distribute liposomal drugs within brain tumors in rat xenograft models[52-54] and canine patients[55] with spontaneous brain tumors. We investigated the distribution and toxicity of DOX-loaded 3-helix micelles delivered by CED to explore their feasibility as a nanocarrier platform for localized delivery in normal rat brain. DOX-loaded micelles showed broader and more even distribution in the brain striatum compared to free DOX, 7 days after infusion (Fig. 5A). It is critical to minimize the intrinsic toxicity from DOX-loaded micelles to normal brain. H&E staining of the harvested brain tissue, a week after infusion, showed that DOX-loaded micelles displayed reduced toxicity, whereas free DOX resulted in significant tissue damage (Fig. 5B). Distribution and toxicity profiles of DOX-loaded micelles indicate stable encapsulation of drug in 3-helix micelles with minimal release in concentrated protein environment of normal brain tissue. These results clearly show that micelles can be locally delivered by CED, and tissue half-life of DOX can be extended with reduced toxicity towards healthy tissue after incorporation in 3-helix micelles. These findings would have significant implications on therapeutic efficacy of drug nanocarriers based on 3-helix micelles delivered by CED for brain cancer.

3.6. Intravenous delivery of DOX-loaded micelles

3-helix micelles with their small size and extended stability present a unique nanocarrier platform for systemic delivery. Intravenous administration of radiolabeled empty 3-helix micelles without drug in NDL tumor bearing mice confirmed significant tumor accumulation (5.7 ± 0.9 % ID/g), comparable to 100 nm, long circulating liposomes (4.3% ID/g).[19] Time dependent PET imaging after tumor localization indicated that 3-helix micelles were highly mobile in tumor tissue, whereas liposomes did not show any detectable movement as function of time, which could be attributed to the significantly smaller size of 3-helix micelles compared to liposomes. The dynamics of nanocarriers in size range of 10-20 nm in tumor could have significant implications on tissue penetration and therapeutic efficacy, which requires further investigation. In the present study, DOX-loaded 3-helix micelles were intravenously administered to NDL tumor bearing FVB mice to investigate the biodistribution of drug loaded micelles. Fig. 6A shows the fluorescence images from different organs, 24 and 72 h after injection of DOX-loaded micelles. Fluorescence in tumor confirms accumulation of DOX-loaded micelles due to EPR effect. Tumor fluorescence increases by 2.1 fold (p value = 0.0028) from 24 to 72 h, whereas, very low fluorescence is detected for other organs during this time period. Fluorescence in different organs at these time points after free DOX injections cannot be detected as clearance time of DOX from

blood circulation is on the order of tens of minutes.[39, 45] The selective fluorescence signal in tumor over extended time period indicates that distribution of DOX in tumor is favorably modified by encapsulation in 3-helix micelles, leading to longer tissue half-life. Thus, incorporation of DOX in 3-helix micelles increases the tumor exposure relative to free drug. Equally important, fluorescence in non-tumor sites including heart, at 24 and 72 h after injection was significantly lower. The fluorescent intensity in heart 24 hours after administration DOX-loaded 3-helix micelles was lower compared to intensity after Doxil administration as quantified previously.[35] These results suggest reduced accumulation of DOX-loaded 3-helix micelles in heart, which is critical to minimize cardiomyopathy associated with DOX. Fig. 6B depicts the images of mouse skin 25 days after administration of DOX-loaded micelles and Doxil. The absence of skin lesions is clearly evident for the mouse treated with DOX-loaded micelles, which indicates that skin toxicity from DOX is significantly reduced after its formulation in 3-helix micelles. On the other hand, accumulation of Doxil in skin increases over time as evident by skin damage.[35] This study focused on evaluation of accumulation of DOX-loaded 3-helix micelles shows that off-target exposure to heart and skin from 3-helix micelles is significantly reduced compared to Doxil, which is encouraging for the safety profile of DOX formulated in 3-helix micelles.

4. Conclusion

In summary, we demonstrate that 3-helix micelles based on amphiphilic peptide-PEG conjugates could incorporate 8 wt% DOX and can be formulated in aqueous buffer in a reproducible manner. The self-assembly of amphiphiles into 15 nm core-shell spherical micelles is maintained after DOX incorporation. DOX-loaded micelles exhibit high stability in terms of size and DOX retention in protein-rich environment similar to conditions after intravenous injections. The disassembly of 3-helix micelles can be triggered by proteolytic degradation of peptide, which allows controlling drug release and clearance to minimize side effects. DOX-loaded micelles exhibit significant toxicity towards a range of cancer cells. *In vivo* studies of intravenous and local administration clearly establish that DOX-loaded micelles improve tissue half-life and reduce off-target toxicity compared to free drug. These findings are encouraging and suggest the potential of 3-helix micelles as a viable nanocarrier platform that meets a number of critical requirements for nanomedicine.

Supplementary Material

Refer to Web version on PubMed Central for supplementary material.

Acknowledgments

N.D. and T.X. were supported by National Institutes of Health under contracts 1R21EB016947-01A1. J.Y.S. was supported by the Office of Basic Energy Sciences, of the U.S. Department of Energy under contract DE-AC02-05CH11231. H.D. was supported by Office of Army of the U.S. Department of Defense under contract W91NF-09-1-0374. J.W.S., E.S., A.K., and K.W.F. were supported by National Institutes of Health under contracts NIHR01CA134659, NIHCA112356 and NIHCA103828. P.Y.C., J.F, and K.B. were supported by funding from UniQure.

References

1. Papahadjopoulos D, Allen TM, Gabizon A, Mayhew E, Matthay K, Huang SK, Lee KD, Woodle MC, Lasic DD, Redemann C. Proc Natl Acad Sci USA. 1991; 88:11460–11464. [PubMed: 1763060]
2. Kwon GS, Kataoka K. Adv Drug Delivery Rev. 1995; 16:295–309.
3. Northfelt DW, Dezube BJ, Thommes JA, Miller BJ, Fischl MA, Friedman-Kien A, Kaplan LD, Du Mond C, Mamelok RD, Henry DH. J Clin Oncol. 1998; 16:2445–2451. [PubMed: 9667262]

4. Gradishar WJ, Tjulandin S, Davidson N, Shaw H, Desai N, Bhar P, Hawkins M, O'Shaughnessy J. J Clin Oncol. 2005; 23:7794–7803. [PubMed: 16172456]
5. Lee CC, MacKay JA, Frechet JMJ, Szoka FC. Nat Biotech. 2005; 23:1517–1526.
6. Duncan R. Nat Rev Cancer. 2006; 6:688–701. [PubMed: 16900224]
7. Matsumura Y. Adv Drug Delivery Rev. 2008; 60:899–914.
8. Matsumura Y, Kataoka K. Cancer Sci. 2009; 100:572–579. [PubMed: 19462526]
9. Elsabahy M, Wooley KL. Chem Soc Rev. 2012; 41:2545–2561. [PubMed: 22334259]
10. Perrault SD, Walkey C, Jennings T, Fischer HC, Chan WCW. Nano Letters. 2009; 9:1909–1915. [PubMed: 19344179]
11. Popović Z, Liu W, Chauhan VP, Lee J, Wong C, Greytak AB, Insin N, Nocera DG, Fukumura D, Jain RK, Bawendi MG. Angew Chem Int Ed. 2010; 49:8649–8652.
12. Cabral H, Matsumoto Y, Mizuno K, Chen Q, Murakami M, Kimura M, Terada Y, Kano MR, Miyazono K, Uesaka M, Nishiyama N, Kataoka K. Nat Nanotech. 2011; 6:815–823.
13. Tang L, Gabrielson NP, Uckun FM, Fan TM, Cheng J. Mol Pharmaceut. 2013; 10:883–892.
14. Chithrani BD, Ghazani AA, Chan WCW. Nano Letters. 2006; 6(4):662–668. [PubMed: 16608261]
15. Jiang W, Kim BYS, Rutka JT, Chan WCW. Nat Nanotech. 2008; 3:145–150.
16. Tang L, Fan TM, Borst LB, Cheng J. ACS Nano. 2012; 6:3954–3966. [PubMed: 22494403]
17. Lee CC, Gillies ER, Fox ME, Guillaudeu SJ, Fréchet JMJ, Dy EE, Szoka FC. Proc Natl Acad Sci USA. 2006; 103:16649–16654. [PubMed: 17075050]
18. MacKay JA, Chen MN, McDaniel JR, Liu WG, Simnick AJ, Chilkoti A. Nat Mater. 2009; 8:993–999. [PubMed: 19898461]
19. Dong H, Dube N, Shu JY, Seo JW, Mahakian LM, Ferrara KW, Xu T. ACS Nano. 2012; 6:5320–5329. [PubMed: 22545944]
20. Dong H, Shu JY, Dube N, Ma Y, Tirrell MV, Downing KH, Xu T. J Am Chem Soc. 2012; 134:11807–11814. [PubMed: 22731391]
21. Lupas AN, Gruber M. Adv Prot Chemistry. 2005; 70:37–78.
22. Apostolovic B, Danial M, Klok HA. Chem Soc Rev. 2010; 39:3541–3575. [PubMed: 20676430]
23. Fox ME, Szoka FC, Fréchet JMJ. Acc Chem Res. 2009; 42:1141–1151. [PubMed: 19555070]
24. Chen H, Kim S, He W, Wang H, Low PS, Park K, Cheng JX. Langmuir. 2008; 24:5213–5217. [PubMed: 18257595]
25. Chen H, Kim S, Li L, Wang S, Park K, Cheng JX. Proc Natl Acad Sci USA. 2008; 105:6596–6601. [PubMed: 18445654]
26. Kastantin M, Missirlis D, Black M, Ananthanarayanan B, Peters D, Tirrell M. J Phys Chem B. 2010; 114:12632–12640. [PubMed: 20828210]
27. Rodrigues PCA, Beyer U, Schumacher P, Roth T, Fiebig HH, Unger C, Messori L, Orioli P, Paper DH, Mülhaupt R, Kratz F. Bioorg Med Chem. 1999; 7:2517–2524. [PubMed: 10632061]
28. Kratz F, Drevs J, Bing G, Stockmar C, Scheuermann K, Lazar P, Unger C. Bioorg Med Chem Lett. 2001; 11:2001–2006. [PubMed: 11454467]
29. Chau Y, Padera RF, Dang NM, Langer R. Int J Cancer. 2006; 118:1519–1526. [PubMed: 16187287]
30. Ogihara NL, Weiss MS, Eisenberg D, Degrado WF. Prot Sci. 1997; 6:80–88.
31. Shu JY, Tan C, DeGrado WF, Xu T. Biomacromolecules. 2008; 9:2111–2117. [PubMed: 18627200]
32. Hadaczek P, Yamashita Y, Mirek H, Tamas L, Bohn MC, Noble C, Park JW, Bankiewicz K. Mol Ther. 2006; 14:69–78. [PubMed: 16650807]
33. Paxinos, G.; Watson, C. The Rat Brain in Stereotaxic Coordinates. Sixth. Elsevier Academic Press; 2005.
34. Miller JK, Shattuck DL, Ingalla EQ, Yen L, Borowsky AD, Young LJT, Cardiff RD, Carraway KL, Sweeney C. Cancer Res. 2008; 68:8286–8294. [PubMed: 18922900]
35. Kheirolomoom A, Mahakian LM, Lai CY, Lindfors HA, Seo JW, Paoli EE, Watson KD, Haynam EM, Ingham ES, Xing L, Cheng RH, Borowsky AD, Cardiff RD, Ferrara KW. Mol Pharmaceut. 2010; 7:1948–1958.

36. Arcamone, F. Doxorubicin : Anticancer Antibiotics. New York Press; 1979.
37. Von Hoff DD, Layard MW, Basa P, Davis JHL, Von Hoff AL, Rozencweig M, Muggia FM. Ann Intern Med. 1979; 91:710–717. [PubMed: 496103]
38. Beijnen JH, van der Houwen OAGJ, Underberg WJM. Int J Pharm. 1986; 32:123–131.
39. Gabizon A, Shiota R, Papahadjopoulos D. J Nat Cancer Inst. 1989; 81:1484–1488. [PubMed: 2778836]
40. Kwon G, Naito M, Yokoyama M, Okano T, Sakurai Y, Kataoka K. J Controlled Release. 1997; 48:195–201.
41. Kataoka K, Matsumoto T, Yokoyama M, Okano T, Sakurai Y, Fukushima S, Okamoto K, Kwon GS. J Controlled Release. 2000; 64:143–153.
42. Shuai X, Ai H, Nasongkla N, Kim S, Gao J. J Controlled Release. 2004; 98:415–426.
43. Gillies ER, Fréchet JMJ. Bioconjug Chemistry. 2005; 16:361–368.
44. Nystrom AM, Xu Z, Xu J, Taylor S, Nittis T, Stewart SA, Leonard J, Wooley KL. Chem Comm. 2008; 30:3579–3581. [PubMed: 18654719]
45. Liu Z, Fan AC, Rakhra K, Sherlock S, Goodwin A, Chen X, Yang Q, Felsher DW, Dai H. Angew Chem Int Ed. 2009; 48:7668–7672.
46. Ren D, Kratz F, Wang SW. Small. 2011; 7:1051–1060. [PubMed: 21456086]
47. Liu J, Xiao Y, Allen C. Polymer-drug compatibility: A guide to the development of delivery systems for the anticancer agent, ellipticine. J Pharm Sci. 2004; 93:132–143. [PubMed: 14648643]
48. Letchford K, Liggins R, Burt H. J Pharm Sci. 2008; 97:1179–1190. [PubMed: 17683080]
49. Lee J, Cho EC, Cho K. J Controlled Release. 2004; 94:323–335.
50. Lin LY, Lee NS, Zhu J, Nyström AM, Pochan DJ, Dorshow RB, Wooley KL. J Controlled Release. 2011; 152:37–48.
51. Yoo HS, Park TG. J Controlled Release. 2001; 70:63–70.
52. Krauze MT, Noble CO, Kawaguchi T, Drummond D, Kirpotin DB, Yamashita Y, Kullberg E, Forsayeth J, Park JW, Bankiewicz KS. NeuroOncol. 2007; 9:393–403.
53. Yamashita Y, T Krauze M, Kawaguchi T, Noble CO, Drummond DC, Park JW, Bankiewicz KS. NeuroOncol. 2007; 9:20–28.
54. Kikuchi T, Saito R, Sugiyama S, Yamashita Y, Kumabe T, Krauze M, Bankiewicz K, Tominaga T. J Neurosurg. 2008; 109:867–873. [PubMed: 18976076]
55. Dickinson PJ, Lecouteur RA, Higgins RJ, Bringas JR, Roberts B, Larson RF, Yamashita Y, Krauze M, Noble CO, Drummond D, Kirpotin DB, Park JW, Berger MS, Bankiewicz KS. J Neurosurg. 2008; 108:989–998. [PubMed: 18447717]

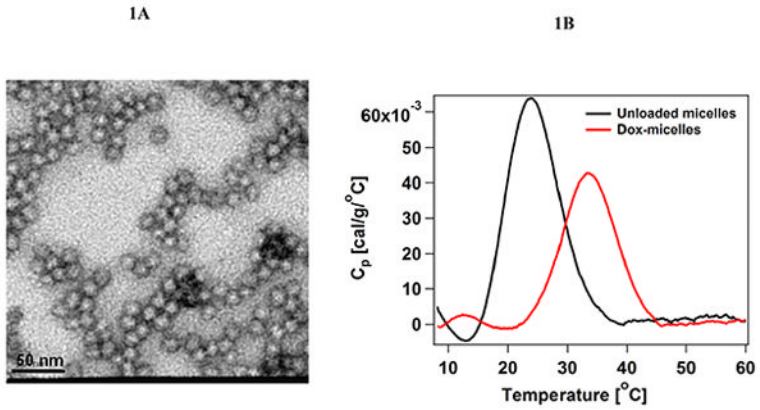

Figure 1.

(A) Negatively stained TEM of DOX-loaded micelles with 8 wt% loading in phosphate buffer (25mM, pH 7.4) showing presence of spherical micelles. (B) DSC thermograms for unloaded and DOX-loaded micelles with 8 wt% loading in phosphate buffer (25mM, pH 7.4), both at concentration of 2 mg/ml. The phase transition temperature for micelle core is increased after DOX encapsulation, which indicates interaction of DOX with alkyl chains in micelle core.

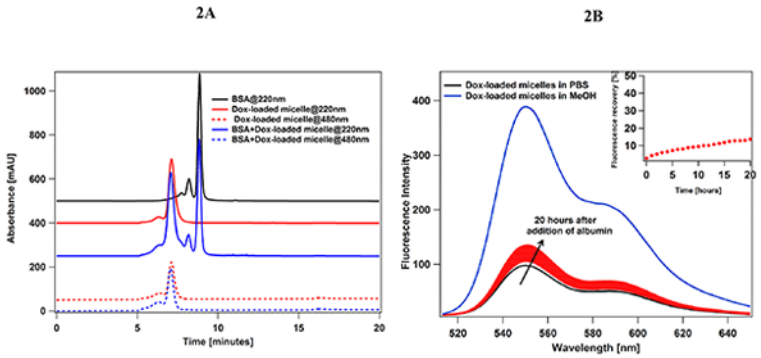

Figure 2.

(A) SEC chromatograms for serum albumin, DOX-loaded micelles and DOX-loaded micelles incubated in serum albumin (10 mg/ml) at 37 °C) for 20 hours. Elution profile at 220 nm monitors the absorbance of albumin and peptide, and elution at 480 nm monitors the absorbance of DOX. Minimal differences were observed in terms of elution profile between DOX-loaded micelles and DOX-loaded micelles after incubation in serum albumin. (B) Drug release from DOX-loaded micelles (DOX concentration, 20 μg/ml) with 8 wt% loading in presence of serum albumin (50 mg/ml, 37 °C) for 20 hours. Emission spectrum of DOX-loaded micelles in phosphate buffer at the start of the experiment indicates quenched fluorescence compared to DOX-loaded micelles in methanol at equivalent concentration. The excitation wavelength is 480 nm and emission spectra are collected from 510-650 nm for 20 hours. Serum albumin is added at the start with final concentration of 50 mg/ml. Inset shows the plot of fluorescence recovery of released drug with respect to florescence of free drug as function of time. Percent recovery is defined as [I(t) – I(0)]/I(MeOH) – I(0)] X100, where I(t) is intensity at time t, I(0) is intensity at $t = 0^-$ before introduction of albumin, and I(MeOH) is intensity in methanol. Intensity values at 550 nm were used for the calculation. I(0) = 97.44, I(MeOH) = 388.58.

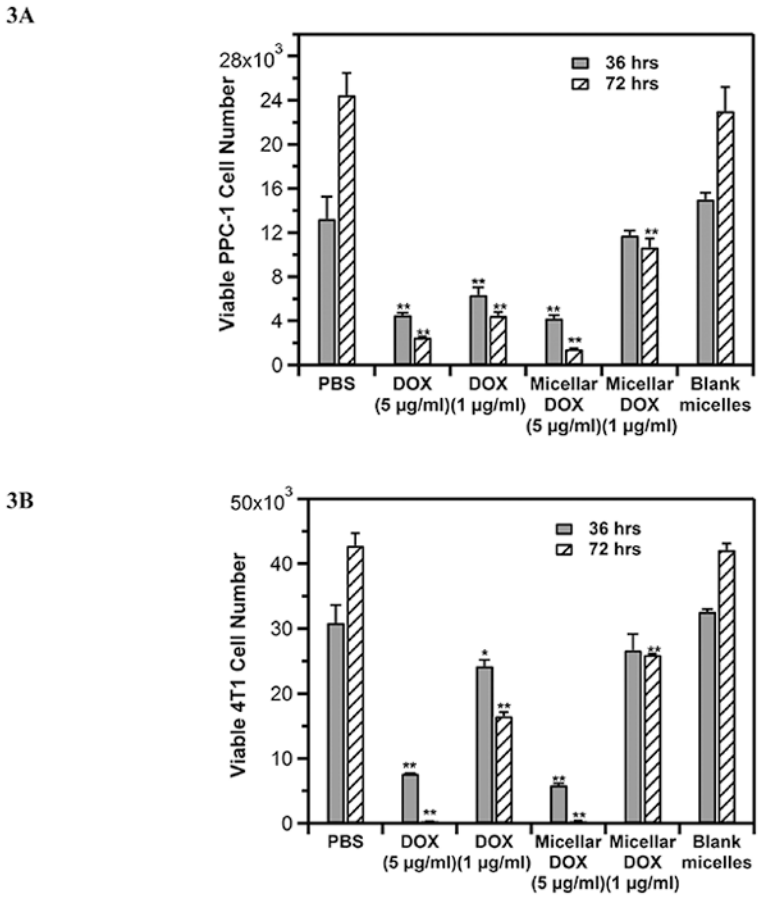

Figure 3.

In vitro cytotoxicity of DOX-loaded micelles for (A) PPC-1 and (B) 4T-1 cancer cells measured by MTT. Both cells were treated with PBS control, free DOX at 5 μg/ml and 1 μg/ml, DOX-loaded micelles at drug concentration of 5 μg/ml and 1 μg/ml and blank micelles with peptide concentration matched to 5 μg/ml DOX-loaded micelles. Viability was evaluated, 36 and 72 hours after treatments. DOX-loaded micelles inhibited the growth of both cells effectively, similar to free drug. Statistical comparisons were performed by ANOVA followed by Tukey's multiple comparisons test. ** $p < 0.0001$ vs. PBS control and blank micelles at the same time point; * $p < 0.05$ vs. PBS control and blank micelles at the same time point.

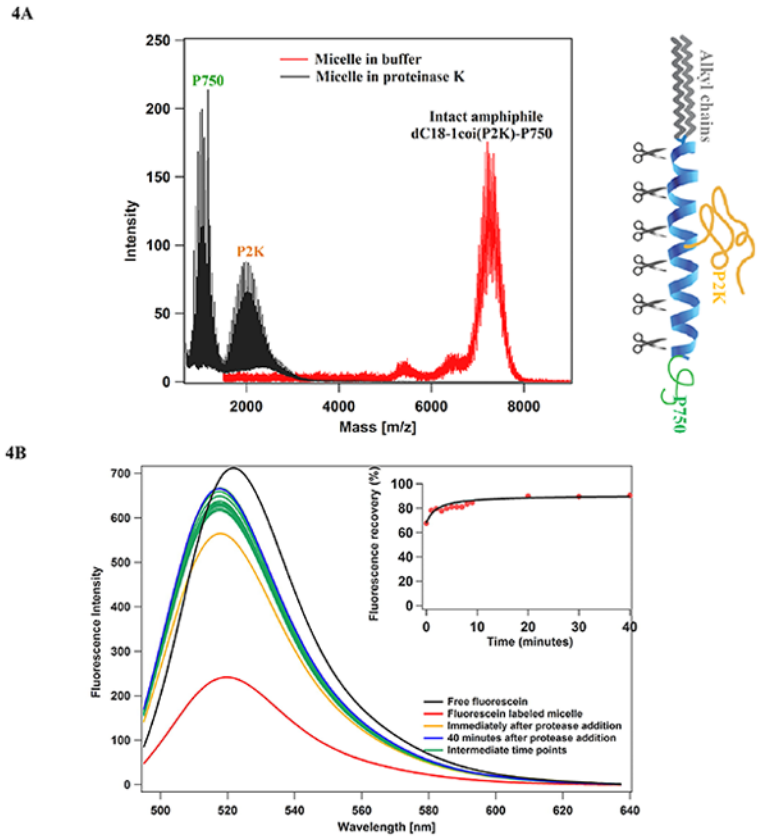

Figure 4.

(A) Schematic of dC18-1coi(P2K)-P750 amphiphile indicating multiple positions at which peptide could be cleaved by proteinase K. MALDI-TOF spectra of the micelle solution before and after incubation with proteinase K, verifying the degradation of the peptide after addition of protease and presence of the PEG2K and PEG750 left after. (B) Emission spectra of fluorescein labeled micelles before and after addition of proteinase K. Self quenching of dye on micelle surface leads to lower fluorescence compared to free dye in solution. After addition of proteinase K (150 μg/ml, phosphate buffer, pH 7.4), fluorescence increases rapidly. The excitation wavelength is 480 nm and emission spectra are collected from 490-650 nm. Inset plots the rate of fluorescence recovery after proteinase K addition and shows very fast increase in fluorescence and indicates micellar disassembly in protease environment.

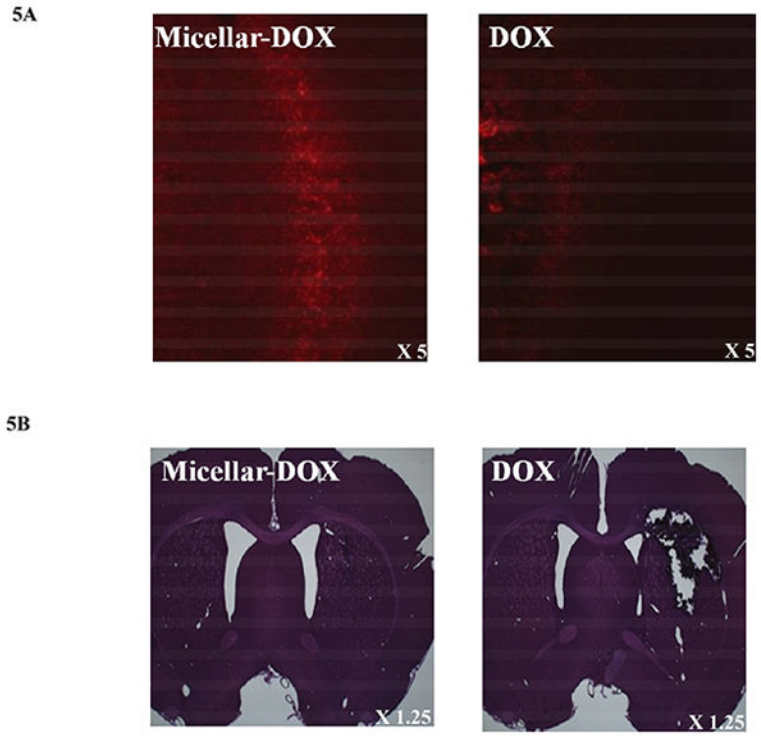

Figure 5.

Brain tissue distribution and toxicity of DOX-loaded micelles and free DOX delivered to Sprague Dawley rats by CED. CED injections were performed at 1 μl/min and total volume injected was 20 μl. DOX concentration for both free and micellar formulation was 0.2 mg/ml. (A) Fluorescence images of striatum 7 days after injection indicate greater distribution of drug in 3-helix micelle formulation. (B) Optical microscopy of tissues after H&E staining, 7 days after injection show significantly lower toxicity from DOX-loaded micelles compared to free DOX.

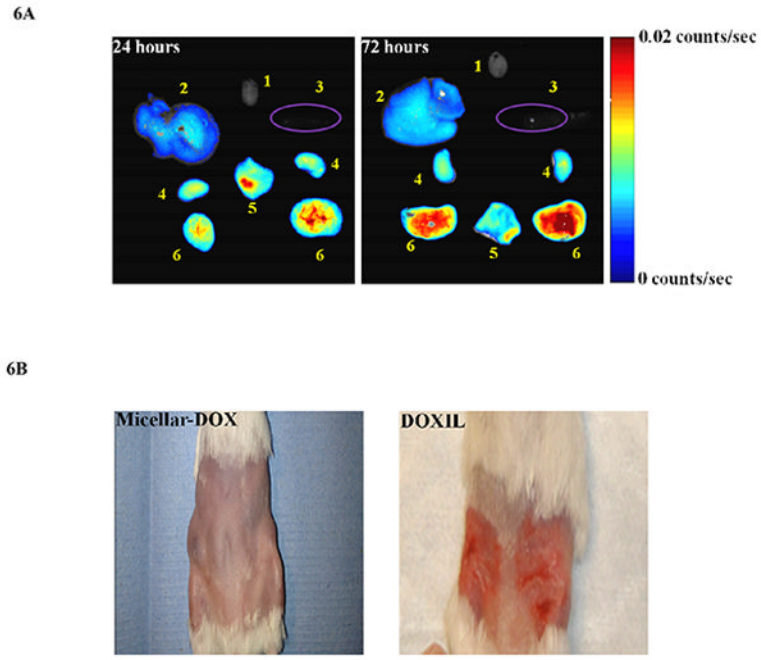

Figure 6.

Biodistribution and toxicity of DOX-loaded micelles after intravenous administration. (A) Fluorescence images of tumor, 24 and 72 hours after injection indicate the presence of DOX fluorescence in tumor for extended period of time. Fluorescence in other organs at these time points is significantly lower, which indicates low accumulation in these organs. The different organs are labeled as 1: heart, 2: liver, 3: spleen, 4: kidney, 5: skin, 6: tumor. (B) Images of mouse skin, 25 days after intravenous injection of DOX-loaded micelles and Doxil, show reduced skin toxicity from DOX-loaded micelles.